DOI: 10.17344/acsi.2018.4419 *Acta Chim. Slov.* **2018,** *65,* 718–729

Scientific paper

Synthesis and Characterization of New Photoresponsive, Ortho and Para Oriented Azomethine Polymers

Farah Qureshi,* Muhammad Yar Khuhawar and Taj Muhammad Jahangir

Institute of Advanced Research Studies in Chemical Sciences, University of Sindh, Jamshoro, Sindh-Pakistan

** Corresponding author: E-mail: farahqureshi94@yahoo.com*
Tel: +92-229213213, +92-3313534844

Received: 20-04-2018

Abstract

Five new azomethine polymers having aliphatic-aromatic moieties were synthesized by polycondensation reaction of dialdehydes and diamines. The dialdehyde monomers differ only in the orientation of the aromatic ring (ortho or para) and were synthesized by condensation reaction between aromatic aldehyde and 1,6-dibromohexane. The molecular mass of the monomers was recorded through E.I mass spectrum. The polymers structures were confirmed by elemental microanalysis, FT-IR, ^{1}HNMR and UV-Vis Spectroscopy. The morphology of monomers and polymers was evaluated by scanning electron microscopy (SEM). All the polymers were soluble in DMSO (on heating) and somewhat in other solvents. Thermal stability of polymers was analyzed by thermogravimetry (TG) and differential thermal analysis (DTA), all the polymers showed good thermal stability higher than their corresponding monomers. The TG of polymers indicated maximum rate of weight loss (T_{max}) within 412–708 °C. Fluorescence emission spectra of polymers were recorded and the results indicated that all the polymers were photo-responsive and indicated 1 to 4 emission bands with maximum within 349–606 nm. The limit of detection of polymers was within 0.625–1.25 μg/ml. The polymers were also examined for their antimicrobial activities against bacteria and fungi.

Keywords: Polyazomethines, thermal stability, fluorescence, antimicrobial activities, morphology

1. Introduction

The conjugated azomethine polymers also called Schiff base polymers are reported and studied since last several decades[1]. These are generally synthesized by polycondensation reaction between dialdehydes or diketones with diamines.[2–4] However, an interest in preparation of new Schiff base polymers and their applications in different field keep on increasing.[5] The researchers are focusing their attention toward conjugated azomethine polymers during recent years[6,7] because of their useful properties such as electrical conductivity, optoelectronic and thermal stability.[8,9] They also exhibit liquid crystalline behavior.[10–14] Poly(azomethines) containing (-N=C) functional group have been applied successfully to some extent as transporting materials in organic solar cells[15–17] and their application.[18] They can act as antimicrobial agents and these are proving interesting, because these are nonvolatile and thermally stable and cannot penetrate through human skin.[19,20] They could protect losses through skin by volatilization.[21,22] The conjugated polyazomethines indicate fluorescence properties, they can be applied in the manufacture of chemical sensors, photoluminescence devices and light emitting diodes.[23,24] The Schiff base polymers derived from aromatic aldehydes with ortho-hydroxy group (salicylaldehyde) can act as chelate polymers with transition metal ions for their removal from industrial contaminated and waste water.[25] The polymeric Schiff bases having aliphatic-aromatic groups indicate better thermal stabilities, but they are difficult to process as they have high melting/ decomposition points and are insoluble in common organic materials.[26] To improve their solubility different arrangements are made in their structure, which includes ether and ester linkages, introducing solution enhancing groups[27] copolymerization and blending.[28–30] Flexible spacers have also been introduced to enhance their solubility without affecting their thermal stability.[31] In the present work five new photo-responsive polyazomethines were synthesized, they differ in orientation of ether groups attached with the aromatic rings and also various types of aromatic or alicyclic rings were incorporated in the polymer chain, the purpose of these structural modifications was to investigate their effects on the properties (solubility, thermal stability and

fluorescence) of polymers. The monomers and their polymers are characterized by different spectroscopic techniques, thermal analysis, scanning electron microscopy (SEM), solubility, spectrofluorimetry and antimicrobial activities.

2. Materials and Methods

2. 1. Materials

2-hydroxybenzaldehyde (Merck, Germany), 4-hydroxybenzaldehyde (Fluka, Switzerland), 1,6-dibromohexane (Sigma Aldrich, St.Louis USA), 2,6-diaminopyridine (Sigma-Aldrich, Germany), 1,4-phenylenediamine (Alfa-Aesar, UK), 1,5-naphthalenediamine (Toshima, Kita-ka, Tokyo, Japan), 1,2-cyclohexanediamine (E.Merck, Germany), dimethylsulfoxide (DMSO) (Daejung, Korea), dimethylformamide (BDH AnalaR, England), anhydrous sodium carbonate (Sigma-Aldrich, Germany), *p*-toluenesulfonic acid (Daejung, Korea), ethanol (E. Merck, Germany), potassium hydroxide (E. Merck, Gerrmany), chloroform, tetrahydrofuran (THF) (E. Merck, Germany) and distilled water from all glass were used.

2. 2. Synthesis of Monomers

Two dialdehyde monomers 2,2'-hexamethylenebis(oxybenzaldehyde) (*o*-HOB) and 4,4'-hexamethylenebis(oxybenzaldehyde) (*p*-HOB) were prepared through the reaction of 2-hydroxybenzaldehyde or 4-hydroxybenzaldehyde with 1,6-dibromohexane by following the reported procedure.[26,31] The preparation of related compounds is also reported[32,33] but in present work procedure reported by Catanescu et al.[26] gave better results and was followed. The mass, FT-IR, ^{1}HNMR and UV spectra of both monomers agreed with the structure assigned and the results are given in Section 3.4, 3.5 and 3.6 respectively. The monomer *o*-HOB indicated m/z (Relative intensity %), M^+ 326 (3.7), 189 (8.9), 147 (14.6), 135 (26.3), 121 (75), 83 (43.8), 55 (100), the mass spectral data of *p*-HOB is already reported.[31]

2. 3. Synthesis of Polymers

The polymers were synthesized by slightly modified general procedure as reported[26,31] as under: A 250 ml round bottom flask equipped with condenser and magnetic stirrer was charged with equimolar mixture (5mmol) of different diamines and dialdehydes, both were dissolved separately in DMF solvent, then *p*-toluenesulfonic acid was added as catalyst. The mixture was refluxed under nitrogen with continuous stirring for 6h. The mixture was poured into 250 ml of water and allowed to form precipitate. The product was collected by filtration, washed with ethanol and dried.

2. 3. 1. *Poly-4,4'-hexamethylenebis (oxybenzaldehyde) 1,5-naphthalenediimine* (P*p*HOBND)

Mp. 280 °C (decomposed), yield 78%, elemental microanalysis calculated for $(C_{30}H_{28}N_2O_2)_n$, (observed %) %C= 80.35(80.68), %H= 6.25 (6.58), %N= 6.25 (5. 42), FT-IR, cm^{-1} (Relative intensity), 2938 (w), 2863 (w), 1668 (m), 1598 (s), 1511 (m), 1472 (w), 1395 (w), 1303 (w), 1249 (S), 1161 (s), 1108 (w), 1015 (w), 925(w), 893 (w), 831(m), 780 (w), 739 (w), 659 (w).^{1}HNMR (DMSO), δ ppm 1.483, 1.764, 4.090 (t), 7.106 (d), 7.841 (d), 9.850. UV (DMSO), λ-max nm (1% absorptivity) 284 (292.4) 340 (60.8).

2. 3. 2. *Poly-4,4'-hexamethylenebis(oxybenzldehyde)1,4-phenylenediimine* (P*p*HOBPD)

Mp. 310 °C (decomposed), yield 76 %, elemental microanalysis calculated for $(C_{26}H_{26}N_2O_2)_n$, (observed %) %C=78.39 (78.29), %H= 6.53 (6.69), %N=7.03 (7.95). FT-IR, cm^{-1} (Relative intensity), 2240(w), 1598 (m), 1570 (w), 1510 (w), 1472 (w), 1422 (w), 1393 (w), 1300 (w), 1242 (s), 1163 (m), 1110 (w), 1017 (m), 950 (w), 883 (w), 835 (m), 766 (w), 724 (w), 655 (w).^{1}HNMR (DMSO), δ ppm 1.227, 1.485, 1.765, 2.720, 2.880, 4.091 (t), 7.106 (d), 7.523, 7.842 (d), 9.851. UV (DMSO), λ-max nm (1% absorptivity) 278 (466.8), 595 (17.2).

2. 3. 3. *Poly-4,4'-hexamethylenebis(oxybenzldehyde)1,2-cycohexanediimine* (P*p*HOBCy)

Mp. 100–200 °C (becomes liquid crystalline at 100 °C and melted at 200 °C), yield 79%, elemental microanalysis calculated for $(C_{26}H_{32}N_2O_2)_n$ (observed %) %C= 77.22 (78.30), %H= 7.92 (8.18), %N= 6.93 (5.58). FT-IR, cm^{-1} (Relative intensity), 2934 (w), 2860 (w) 1683 (m), 1640 (m) 1601 (m), 1511 (m), 1470 (w), 1389 (w), 1306 (w), 1246 (s), 1160 (m), 1111 (w), 1084 (w), 1013 (m), 946 (w), 839 (m), 746 (w), 712 (w), 683 (w), 658 (w). ^{1}HNMR (DMSO), δ ppm 1.208, 1.238, 1.270, 1.295, 1.319, 1.346, 1.386, 1.482, 1.539, 1.568, 1.602, 1.755 (d), 1.839, 3.998, 4.089 (t), 6.854 (d), 6.945 (d), 7.104 (d), 7.501 (d), 7.601 (t), 7.758 (d), 7.841 (d), 8.168 (d), 9.850. UV (DMSO), λ-max nm (1% absorptivity) 275 (434.2)

2. 3. 4. P*oly-2,2'-hexamethylenebis(oxybenzldehyde)1,4-phenylenediimine* (P*o*HOBPD)

Mp. 150 °C (decomposed), yield 75%, elemental microanalysis calculated for $(C_{26}H_{26}N_2O_2)_n$ (observed %) %C= 78.39 (78.34), %H= 6.53 (6.63), %N= 7.03 (6.97). FT-IR, cm^{-1} (Relative intensity), 2943 (w), 2868 (w), 1685 (w), 1611 (m), 1595 (s), 1497 (m), 1485 (w), 1479 (w), 1456 (m), 1396 (w), 1364 (w), 1301 (w), 1286 (w), 1249 (s), 1187 (w), 1160 (w), 1102 (m), 1043 (w), 1021 (m), 980 (w), 887 (w), 839 (m), 780 (w), 750 (s), 730 (w). ^{1}HNMR (DMSO), δ ppm 1.228, 1.534, 1.802, 2.722, 2.882, 4.132 (d), 7.050,

7.214 (d), 10.379. UV (DMSO), λ-max nm (1% absorptivity) 262 (660.8), 321 (542.4), 373 (465.6)

2. 3. 5. *Poly-2,2'-hexamethylenebis(oxybenzldehyde)2,6-diiminopyridine* (PoHOBP)

Melting/decomposition above 360 °C, yield 76 %, elemental microanalysis calculated for $(C_{25}H_{25}N_3O_2)_n$ (observed %) %C= 75.18 (75.02), %H= 6.26 (6.70), %N= 10.52 (10.22). FT-IR, cm^{-1} (Relative intensity), 3620 (w), 2940 (w), 2862 (w), 2219 (w), 1681(w), 1596 (m), 1483 (w), 1449 (s), 1284(w), 1233 (s), 1160 (w), 1102 (w), 1044 (w), 999 (w), 930 (w), 869 (w), 833 (w), 800 (w), 834 (m), 751 (s), 720 (w), 683 (w), 647 (w). ^{1}HNMR (DMSO), δ ppm 1.225, 1.532, 1.799, 1.815, 2.720, 2.879, 4.136 (t), 7.029, 7.048, 7.067, 7.202, 7.224, 7.610, 7.629, 7.658 (d), 7.677 (d), 7.941, 10.377. UV (DMSO), λ-max nm (1% absorptivity) 261 (122.4), 320 (80.8).

2. 4. Analysis of Monomers and Polymers.

The elemental microanalysis of polymers was performed by elemental microanalysis Ltd, Devon, United Kingdom. E.I mass spectra of the monomers were recorded on JEOL JMS 600 mass spectrometer (USA) at HEJ Research Institute of Chemistry, University of Karachi, Sindh-Pakistan. UV-Vis spectra of monomers and polymers were recorded in DMSO solvent within 500–200 nm on Perkin Elmer double beam Lambda 35 spectrophotometer (Perkin Elmer, Singapur) using dual 1 cm quartz cuvette. Spectrophotometer was controlled by the computer with software. FT-IR spectra of the synthesized compounds were recorded within 4000–600 cm^{-1} on Nicolet Avatar 330 FT-IR with Attenuated total reflectance (ATR) accessory (smart partner) (Thermo Scientific, USA). ^{1}HNMR spectra of the compounds were recorded on Bruker AVANCE-NMR spectrophotometer (UK) at 400 MHz using tetramethylsilane (TMS) as internal standard and DMSO as solvent at HEJ Research Institute of Chemistry, University of Karachi Sindh-Pakistan. Fluorescence measurement was performed on Spectrofluorophotometer RF-5301 PC Series (Shimadzu Corporation, Kyoto, Japan) using 1cm quartz cuvette. Thermogravimetry (TG) and Differential thermal analysis (DTA) were performed at Centralized Resource Laboratory, University of Peshawar, Peshawar-Pakistan on thermogravimetric thermal analyzer Pyris Diamond TG/DTA (Perkin Elmer, USA) in nitrogen atmosphere with a flow rate of 50 ml/min and heating rate of 20 °C /min from 50 °C to 800 °C using 5 to 9 mg of sample placed on ceramic pan. In order to determine the morphologies of polymers they were also characterized by Scanning electron microscopy using JEOL JSM-6490LV Scanning Electron Microscope (USA) at Center for Pure and Applied Geology, University of Sindh, Jamshoro, Sindh-Pakistan. The accelerating voltage for taking images was 15 KV.

The antibacterial activity of the polymers was measured through 96 well plate method by using microplate alamar blue assay. The antibacterial activity was tested against bacterial species: Escherichia coli, Shigella flexenari, Staphylococcus aureus, and Pseudomonas aeruginosa using standard drug Ofloxacin. For measuring antifungal activity of the polymers agar tube dilution method was used. The antifungal activity was tested against fungal species: Trichphyton rubrum, Candida albicans, Aspergillus nigar, Microsporum canis, Fusarium lini, Canadida gla-

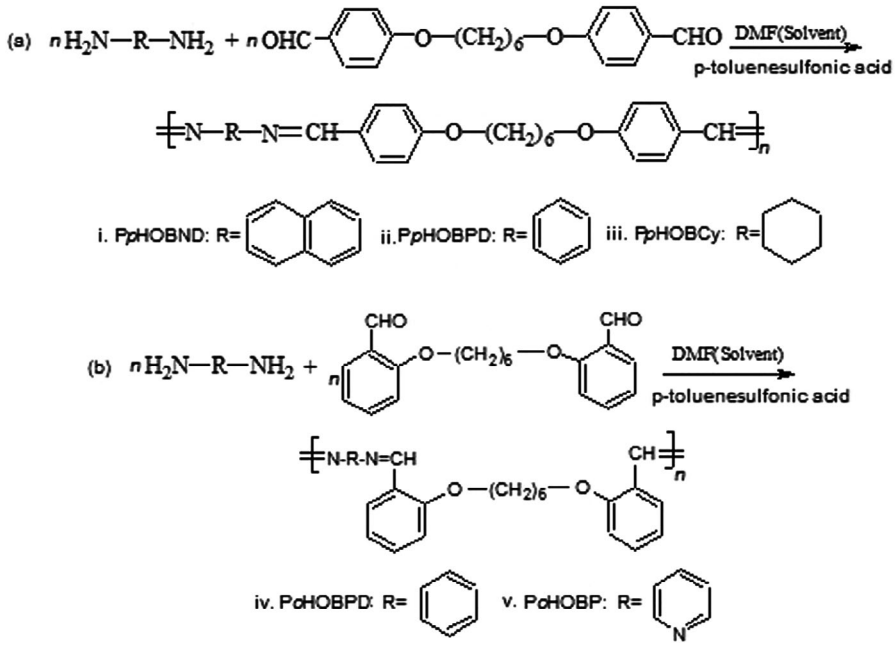

Scheme 1. Reaction scheme (a) synthesis of para oriented polymers (b) synthesis of ortho oriented polymers.

brata using standard drug Amphotericin B for Aspergillus nigar and drug Miconazole for other species. Percent inhibition of the polymers was compared with the percent inhibition of the standard drug. For antibacterial assay 2 mg of polymer was dissolved in DMSO solvent to get concentration of 50 µg/ ml. For antifungal assay the concentration of polymers was 200 µg/ ml in DMSO. Incubation period was 7 days at 28 °C ± 1 °C.

3. Results and Discussion

3. 1. Synthesis of Monomers and Polymers

The dialdehyde monomers (*p*-HOB or *o*-HOB) were prepared by condensation of *p*-hydroxybenzaldehyde or *o*-hydroxybenzaldehyde with 1,6-dibromohexane. The monomers were obtained in good yield, *p*-HOB = 92% and *o*-HOB=81%. The aliphatic spacers of n-hexane are common in both the (dialdehyde) monomers. The variation is only in the ortho and para linkages. The polycondensation of an equimolar mixture of dialdehyde (*p*-HOB or *o*-HOB) with diamines (1,5-naphthalenediamine, 1,4-phenylenediamine, 1,2-cyclohexanediamine, 2,6-diaminopyridine) results into polymers (P*p*HOBND, P*p*HOBPD, P*p*HOBCy, P*o*HOBPD or P*o*HOBP) containing aliphatic-aromatic groups in the main chain following the reaction Scheme 1. The polymers were also obtained in good yield (76–79%). The structure of the polymers was confirmed by different techniques and the results supported their formation. Salih İlhan et al. have reported the formation of Schiff base by the condensation of monomer *o*-HOB with 2,6-diaminopyridine.[34] Similar reactants were used for the synthesis of polymer P*o*HOBP, the melting/decomposition point of the polymer (P*o*HOBP) was above 360 °C while the reported Schiff base decomposed at 280 °C, the mass spectrum of the polymer (P*o*HOBP) obtained through E.I mass spectroscopy did not show the mass corresponding to Schiff base, the polymer (P*o*HOBP) had higher mass than the reported Schiff base which supported the formation of the polymer (P*o*HOBP).

Table 1. Solubility of monomers and polymers in different solvents at the concentration of 5mg/ 5 ml

S. No	Compound	Solubility in different solvents					
		H_2O	Ethanol	Chloroform	THF	DMF	DMSO
1.	*p*-HOB	IS[e]	S[a]	S	S	S	S
2.	P*p*HOBND	IS	IS	IS	PS[c]	PS	S(Δ)[b]
3.	P*p*HOBPD	IS	IS	IS	IS	IS	S(Δ)
4.	P*p*HOBCy	IS	PS	IS	IS	PS	S
5.	*o*-HOB	IS	S	S	S	S	S
6.	P*o*HOBPD	IS	IS	SS[d]	IS	IS	S(Δ)
7.	P*o*HOBP	IS	IS	IS	IS	PS	S(Δ)

[a](soluble), [b](soluble on heating), [c](partially soluble), [d](slightly soluble), [e](insoluble)

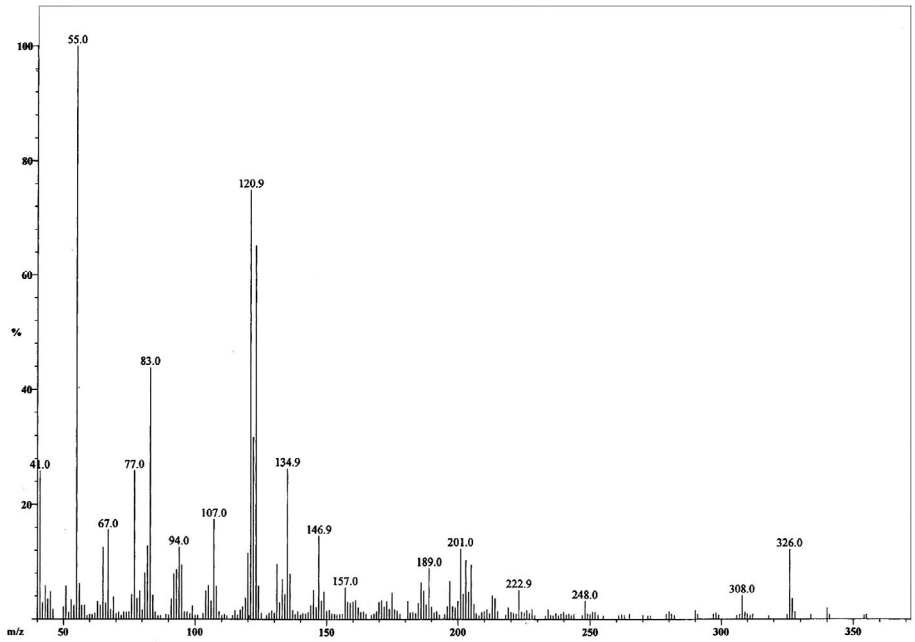

Figure 1. E.I mass spectrum of the monomer *o*-HOB

3. 2. Solubility of Monomers and Polymers

The solubility of monomers and polymers is summarized in Table 1. The monomers were soluble in organic solvents and insoluble in water. The polymers were soluble in DMSO on heating but the P*p*HOBCy was soluble in DMSO without heating also. The better solubility of P*p*HOBCy is because of the presence of more flexible cyclohexane ring while other synthesized polymers have rigid aromatic rings.

3. 3. E.I Mass Spectrum of Monomers

The mass spectrum of *p*-HOB is already reported[31] and the mass spectrum of *o*-HOB showed M^+ at m/z 326, and other main fragments at m/z 205, 189, 177, 147, 135 and 121 corresponding to $[M\text{-}(O.C_6H_4.CHO)]^+$, $[CHO.C_6H_4.O.(CH_2)_3.CH{=}CH]^+$, $[CHO.C_6H_4.O.(CH_2)_4]^+$, $[CHO.C_6H_4.O.\ CH{=}CH]^+$, $[CHO.C_6H_4.O.CH_2]^+$ and $[CHO.C_6H_4.O]^+$. The peaks at 83(43%) and 55(100%) corresponded to C_6H_{11} and C_4H_7 as shown in Figure 1.

3. 4. FT-IR of Monomers and Polymers

FT-IR of *p*-HOB is reported[31] and the FT-IR of *o*-HOB also agreed with the reported values[34]. The comparative FT-IR of *p*-HOB and *o*-HOB showed as under: monomer *p*-HOB and *o*-HOB showed strong band at 1685 cm^{-1} and 1678 cm^{-1} for υ C=O respectively, *p*-HOB shows bands at 1595, 1507 cm^{-1} and *o*-HOB at 1595, 1484 cm^{-1} for υ C=C aromatic rings. The *p*-HOB showed bands at 1250, 1069 cm^{-1} and *o*-HOB at 1244, 1072 cm^{-1} for C-O-C vibrations. The polymers P*p*HOBND, P*o*HOBPD and P*o*HOBP showed weak band while P*p*HOBCy indicated medium intensity band within 1668–1682 cm^{-1}due to υ C=O of end on groups but this band was not visible in P*p*HOBPD. The polymers indicated band of strong to medium intensity within 1596–1640 cm^{-1}due to υ C=N. One to two bands were visible within 1601–1482 cm^{-1} due to aromatic rings of the polymers. The polymers show band within 1233–1249 due to C-O-C asymmetric vibrations and a band within 999 to 1021 due to C-O-C symmetric vibrations. The polymers spectra showed number of band within 980–646 cm^{-1} due to in plane and out of plane C-H vibration of aromatic rings as shown in Figure 2**.** Similar assignments have been indicated for FT-IR of polyazomethines[8].

3. 5. ^{1}HNMR Spectroscopy of Monomers and Polymers

The ^{1}HNMR of monomer *p*-HOB[31] and ^{13}C-NMR of *o*-HOB[34] are reported. The comparative ^{1}HNMR (DMSO) spectra of monomers indicated δ ppm for *p*-HOB at 9.850 and *o*-HOB at 10.375 for CHO, *p*-HOB indicated two doublets at 7.840 and 7.103 while *o*-HOB indicated multiplet at 7.641, doublet at 7.208, and triplet at 7.044 due to C-H aromatic protons. The *p*-HOB indicated triplet at 4.089 while *o*-HOB indicated triplet at 4.130 for O-CH_2 groups. *p*-HOB indicated triplet at 1.746 and singlet at 1.482 while *o*-HOB indicated doublet at 1.803 and

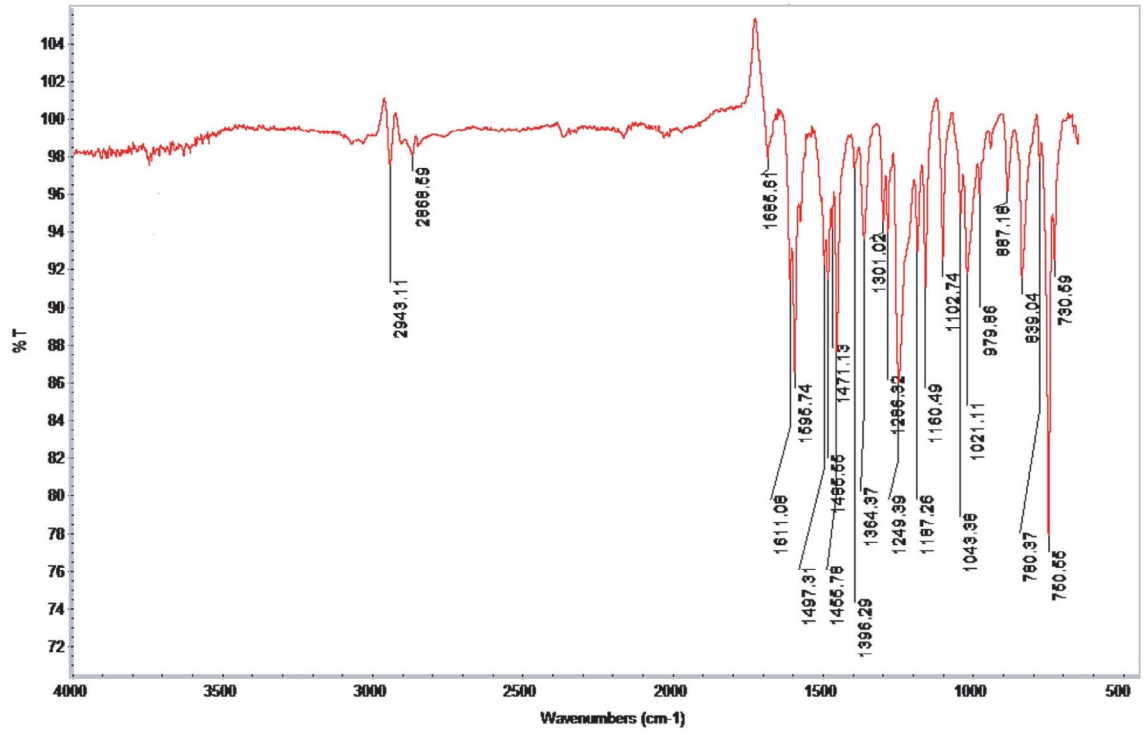

Figure 2. FT-IR spectrum of polymer P*o*HOBPD, conditions as experimental

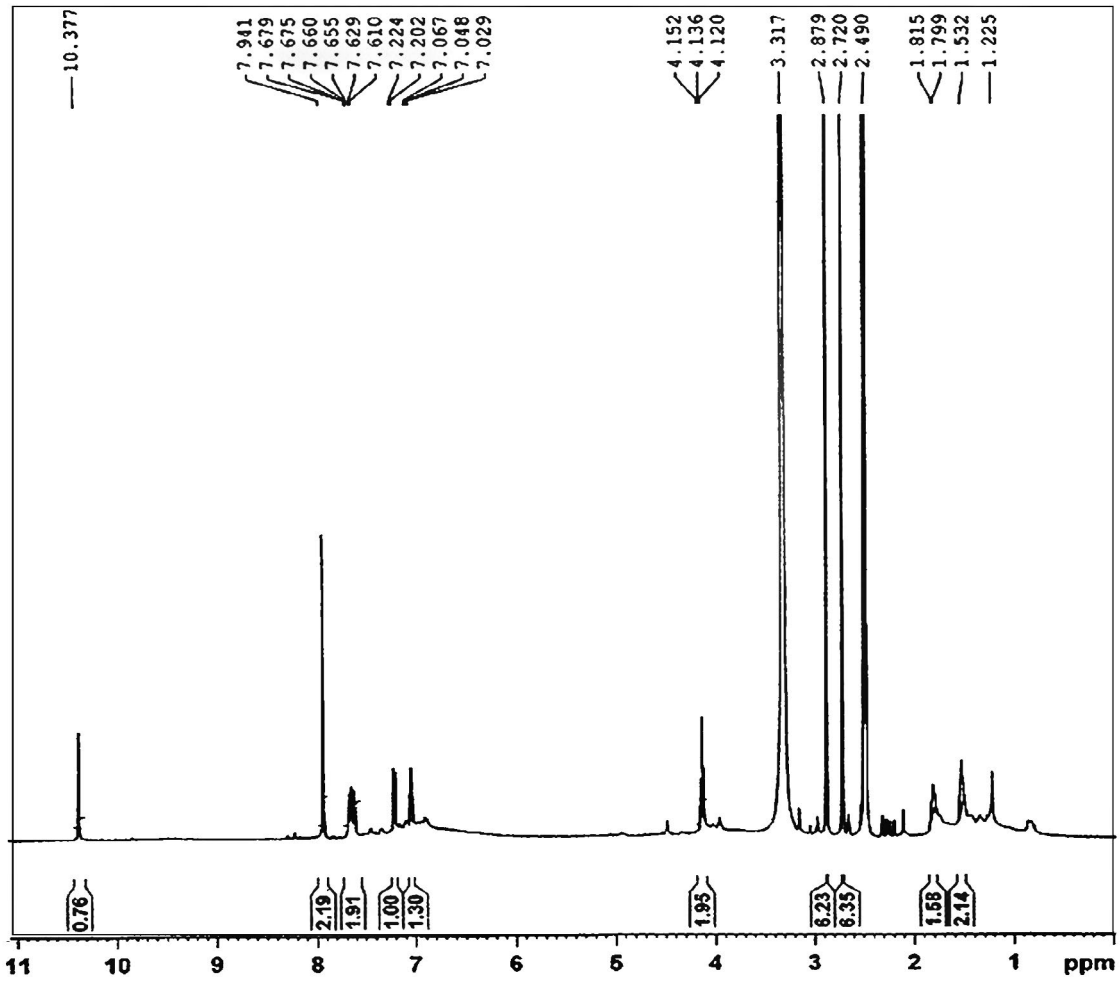

Figure 3. [1]HNMR spectrum of polymer P*o*HOBP

singlet at 1.527 for CH_2 groups, Catanescu et al have reported a similar assignments for related monomer.[26] [1]HNMR in DMSO of the polymer P*p*HOBND showed singlet at δ ppm 9.850 for N=CH/HC=O, two doublets at 7.106 and 7.841 for C-H aromatic protons, triplet at 4.090 for O-CH_2 and singlet at 1.764 and 1.483 for CH_2 groups. P*p*HOBPD indicated singlet at 9.851 for N=CH/HC=O, doublet at 7.106, singlet at 7.523 and doublet at 7.842 for aromatic C-H protons, triplet at 4.091 for O-CH_2 and singlets at 2.880, 2.720, 1.765, 1.485, 1.227 for CH_2 groups. P*p*HOBCy indicated singlet at δ ppm 9.850 for N=CH/HC=O, doublets at 8.168, 7.841, 7.758, triplet at 7.601 and doublets at 7.501, 7.104, 6.945, 6.854 for aromatic C-H protons, triplet at 4.089 for O-CH_2 groups, singlet at 3.998 was for cyclohexane, singlet at 1.839, doublet at 1.755 and singlets at 1.602, 1.568, 1.539, 1.482, 1.386, 1.346, 1.319, 1.295, 1.270, 1.238, 1.208 for CH_2 groups (n-hexane or cyclohexane CH_2 protons). P*o*HOBPD showed singlet at 10.379 for N=CH, doublet at 7.214 and singlet at 7.050 for C-H aromatic protons, doublet at 4.132 for O-CH_2 and singlet from 2.882 to 1.228 for CH_2 groups. P*o*HOBP indicated singlet at 10.377 for N=CH, singlet at 7.941, doublets at 7.677, 7.658, singlets from 7.629 to 7.029 for C-H aromatic protons, triplet at 4.136 for O-CH_2, singlets from 2.879, 2.720, 1.815, 1.799, 1.532, 1.225 for CH_2 groups (Figure 3).

3. 6. UV-Vis Spectroscopy of Monomers and Polymers

UV-Vis spectra of monomers and polymers were obtained in DMSO. The monomer *p*-HOB shows a broad band at 283 nm and its molar absorptivity was 3.2×10^4 L.mole^{-1} cm^{-1}. The monomer *o*-HOB shows two bands at 258 nm and 322 nm with molar absorptivities 1.5×10^4 and 8.8×10^3 L mole^{-1} cm^{-1}. The polymers P*p*HOBND, P*p*HOBPD and P*o*HOBP showed two bands while polymer P*o*HOBPD showed three bands (Figure 4), the increase in the number of bands in the absorption spectra is due to π-π* transition in conjugated azomethine with naphthalene, phenyl and pyridine rings. The polymer P*p*HOBCy showed only one band because extension of conjugation was not possible with cyclohexane ring. The results are summarized in Table 2.

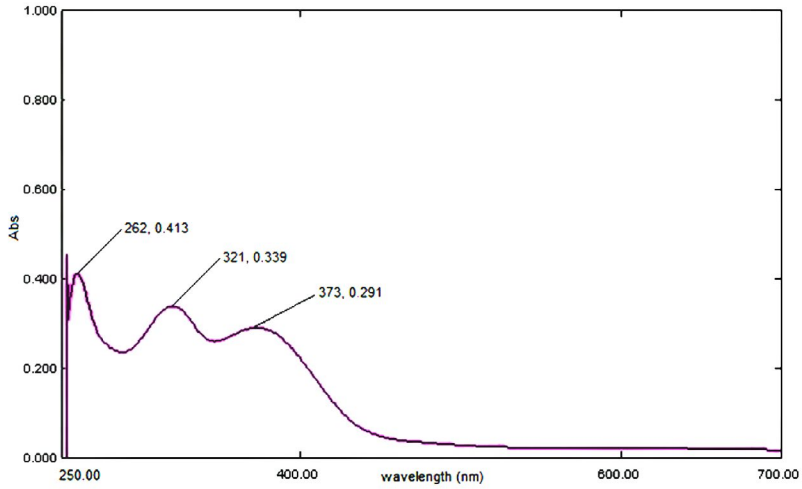

Figure 4. UV/Vis spectrum of the polymer P*o*HOBPD conditions as experimental

Table 2. Results of spectrophotometric studies of monomers and polymers in DMSO Solvent

S. No	Compound	λ nm (ε 1%)	Possible transition
1.	*p*-HOB	283(32500)[a]	π – π* transition within aromatic ring system
2.	*o*-HOB	258(15987)[a]	π – π* transition within aromatic ring system
		322(8867)[a]	π – π* transition involving aromatic ring and conjugated C=C-C=O π-electron system
3.	P*p*HOBND	284(292)	π – π* transition within aromatic ring system
		340(61)	π – π* transition involving aromatic ring and conjugated C=C-N=C π-electron system
4.	P*p*HOBPD	278(467)	π – π* transition within aromatic ring system
		595(17)	π – π* transition in conjugated azomethine group
5.	P*p*HOBCy	275(434)	π – π* transition within aromatic ring system
6.	P*o*HOBPD	262(661)	π – π* transition within aromatic ring system
		321(542)	π – π* transition involving aromatic ring and conjugated C=C-N=C π-electron system
		373(466)	π – π* transition in conjugated azomethine group
7.	P*o*HOBP	261(122)	π – π* transition within aromatic ring system
		320(81)	π – π* transition involving aromatic ring and conjugated C=C-N=C π-electron system

[a](molar absorptivity (ε) L. mol^{-1} cm^{-1})

3. 7. Fluorescence Spectroscopy of Monomers and Polymers

The monomers and polymers contained conjugated chromophoric groups which could indicate fluorescence intensity within UV-Vis region. Choi et al.[24] have reported fluorescence from poly(azimethines). Fluorescence emission of the monomers and polymers were examined in DMSO solvent. The monomer *p*-HOB showed a emission band at 378 (at excitation 275 nm) and *o*-HOB shows two emission bands 354 nm (excitation 258 nm) and 374 nm (excitation 322 nm). The polymers indicated two to four emission bands (Figure 5), except P*p*HOBCy which indicated one emission band at 349 nm (excitation 275 nm). The results of spectrofluorometric studies are summarized in Table 3, and the results showed that all the monomers and the polymers were fluorescence materials. The polymer P*p*HOBND indicated highest fluorescence intensity and P*p*HOBCy indicated lowest intensity. There was a shift in wavelength of emission and excitation of the polymers as compared to their corresponding monomers *p*-HOB and *o*-HOB due to polymerization. The number of emission bands observed were higher (3 and 4) for the polymers P*o*HOBPD and P*o*HOBP derived from *o*-HOB as compared to the polymers P*p*HOBND, P*p*HOBPD and P*p*HOBCy (1 to 2 emission bands) derived from the mon-

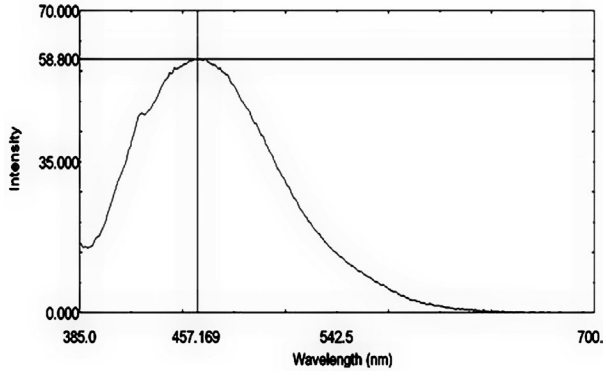

Figure 5. Fluorescence emission spectrum of polymer P*o*HOBPD (λex: 373 nm, λem: 457 nm)

Table 3: Spectrofluorometric determination of monomers and polymers using DMSO solvent

S. No	Compound	Concentration in μg/ml	Excitation wavelength in nm	Emission wavelength in nm (color)	Relative Intensity of emission
1.	*p*-HOB	20	283	375	948
2.	*o*-HOB	12.5	258	354	76.2
			322	374	178.1
3.	P*p*HOBND	25	284	372	409
			340	399 (violet)	1018
4.	P*p*HOBPD	25	278	351	355
			595	688 (red)	18.1
5.	P*p*HOBCy	50	275	349	5.45
6.	P*o*HOBPD	6.25	262	354	204.2
			321	388 (violet)	261.4
			373	457 (blue)	58.80
7.	P*o*HOBP	25	261	353	232
				434 (violet)	105.6
				526 (green)	29.5
			320	357	273.5

omer *p*-HOB due to ortho group effect. All the polymers showed 1 or 2 color emissions except P*p*HOBCy, the emission colors include violet, blue, green and red. The limit of detection (LODs) of the polymers in DMSO were calculated, at least signal to noise ratio 3:1 at the emission band of higher sensitivity and were observed within 0.625–1.25 μg/ml.

3. 8. Thermal Analysis of Monomers and Polymers

Thermal behavior of monomer and polymers was evaluated by TG (Thermogravimetry) and DTA (Differential thermal analysis) in nitrogen atmosphere. TG and DTA of monomer *p*-HOB is reported.[31] TG of *o*-HOB showed three stages of weight loss with 73% weight loss within 216–465 °C, 6% weight loss within 466–542 °C and 15% weight loss within 543–625 °C with maximum rate of weight loss (T_{max}) at 357 °C, DTA showed melting endotherm at 93 °C, followed by vaporization/decomposition exotherms at 403, 464 and 532 °C and large decomposition exotherm at 603 °C. TG of P*p*HOBND showed four stages of weight loss with 6% weight loss within 300–426 °C, 37% weight loss within 427–520 °C, 6% weight loss within 521–605 °C and 48% weight loss within 606–795 °C, T_{max} indicated at 708˚C, DTA showed two exotherms at 416 and 466˚C due to vaporization/decomposition and large decomposition exotherm at 714˚C. TG of P*p*HOBPD showed two stages of weight loss with 28% weight loss within 363–500 °C and 66% weight loss within 501–705 °C with T_{max} at 628 °C, DTA showed two large decomposition exotherms at 398 and 615 °C. TG of P*p*HOBCy showed four stages of weight loss with 22% weight loss within 280–425 °C, 40 % weight loss within 426–500 °C, 8 % weight loss within 501–555 °C and 22% weight loss within 556–626 °C with T_{max} at 469 °C (the lower T_{max} value was may be due to the presence of cyclohexane ring), DTA showed two decomposition exotherms at 366 and 470 °C, and a large decomposition exotherm at 596 °C. TG of P*o*HOBPD showed three stages of weight loss with 44% weight loss within 346–477 °C, 9% weight loss within 478–558 °C and 38% weight loss within 559–674 °C, T_{max} value showed at 412 °C, DTA indicated three vaporization/decomposition exotherms at 395, 463 and 517 °C, followed by large decompo-

Table 4. Thermal analysis data of monomers and polymers

Compound	TG analysis Weight loss stages I	II	III	IV	Thermal stability	DTA analysis	
	Wt. loss % (temperature range °C)				T_{max} °C	Endo ˚C	Exo °C
p-HOB	95 (250–500)	–	–	–	362	112, 365, 475	
o-HOB	73 (216–465)	6 (466–542)	15 (543–625)	–	357	93	403, 464, 532, 603
P*p*HOBND	6 (300–426)	37 (427–520)	6 (521–605)	48 (522–795)	708	–	416, 466, 714
P*p*HOBPD	28 (363–500)	66 (501–705)	–	–	628	–	398, 615
P*p*HOBCy	22 (280–425)	40 (426–500)	8 (501–555)	22 (556–626)	469	–	366, 470, 596
P*o*HOBPD	44 (346–477)	9 (478–558)	38 (559–674)	–	412	–	395, 463, 517, 661
P*o*HOBP	8 (99–338)	28 (339–480)	11 (481–574)	49 (575–743)	655	–	358, 448, 514, 684

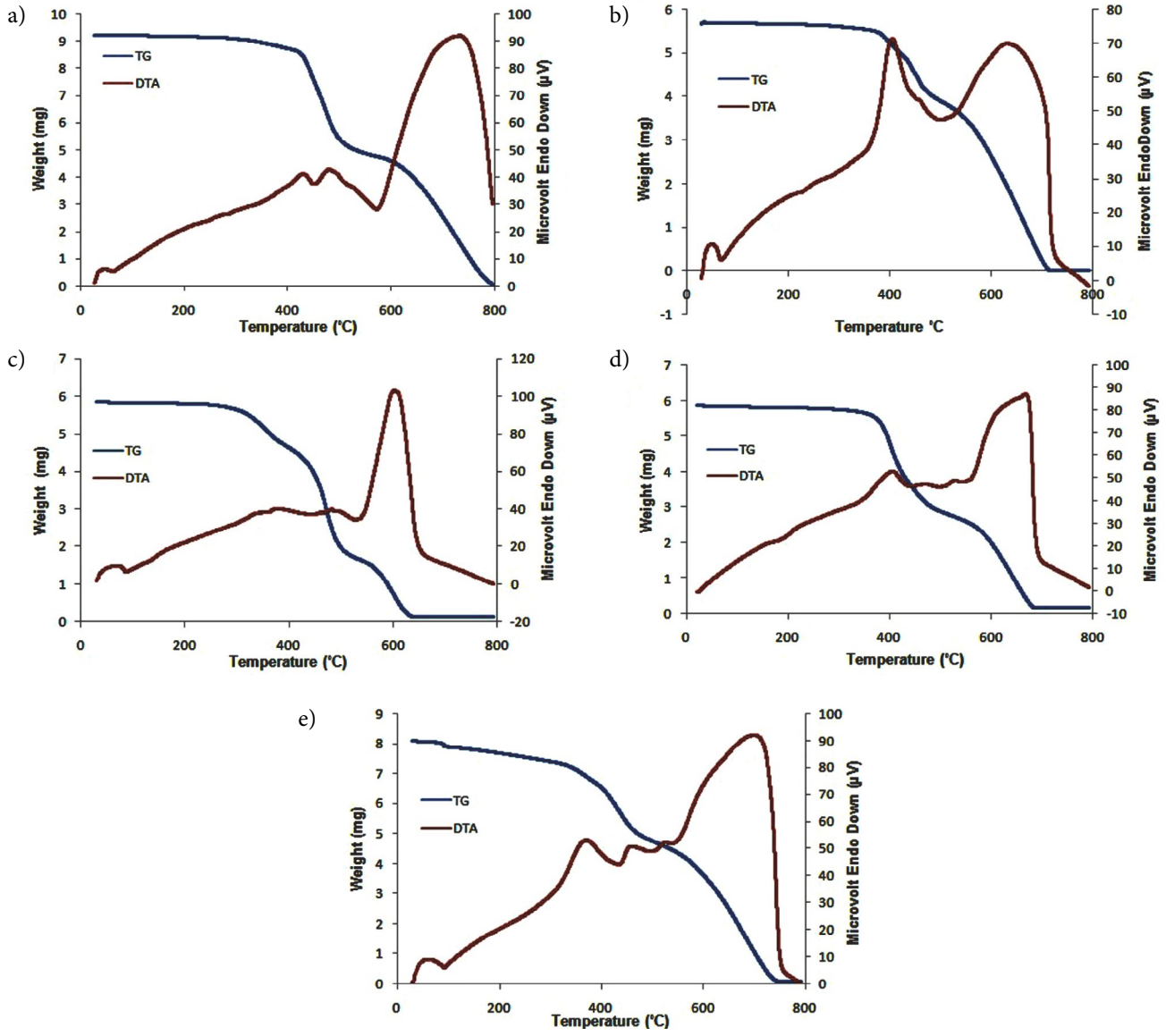

Figure 6. TG/DTA graphs of polymers (a) P*p*HOBND (b) P*p*HOBPD (c) P*p*HOBCy (d) P*o*HOBPD and (e) P*o*HOBP conditions as experimental

sition exotherm at 661 °C. TG of P*o*HOBP indicated four stages of weight loss with 8% weight loss within 99–338 °C, 28% weight loss within 339–480 °C, 11% weight loss within 481–574 °C and 49% weight loss within 575–743 °C with T_{max} at 655 °C, DTA showed three vaprization/decomposition exotherms at 358, 448 and 514˚C and a large decomposition exotherm at 684˚C. The TG/DTA graphs of all the polymers are given in Figure 6. The polymers indicated high thermal stability as compared to monomers because their T_{max} values were higher than their corresponding monomers. The thermal analysis results are given in Table 4.

3. 9. Biological Activities of Polymers

The polymers were tested for their biological activities against bacteria and fungi. The polymer P*p*HOBND showed 40% antifungal activity against Aspergillus nigar, P*p*HOBPD showed 30% inhibition against Fusarium Lini, P*p*HOBCy indicated 20% inhibition against Candida albicans, P*o*HOBPD showed 15% inhibition against Microsporum canis while the polymer P*o*HOBP did not showed inhibition against fungi, the results of antifungal activities are summarized in Table 5. The polymer P*p*HOBCy indicated 22% antibacterial activity against staphylococcus aureus and 3.24% inhibition against Escherichia Coli, P*o*-HOBPD showed 18.6% inhibition against staphylococcus aureus, P*p*HOBND showed 11% inhibition against Escherichia Coli and 9% inhibition against staphylococcus aureus, P*p*HOBPD showed 7.18% inhibition against Escherichia Coli and 4.53% inhibition against staphylococcus aureus and the polymer P*o*HOBP showed 8.86% inhibition against Escherichia Coli, the results of antibacterial activities are summarized in Table 6.

Table 5: Results of antifungal activities of polymers in DMSO solvent

Name of Fungus	% inhibition of Polymers				Standard Drug
	P*p*HOBND	P*p*HOBPD	P*p*HOBCy	P*o*HOBPD	
Trichphyton rubrum	–	–	–	–	Miconazole
Candida albicans	–	–	20%	–	Miconazole
Aspergillus nigar	40%	–	–	–	Amphotericin B
Microsporum canis	–	–	–	15%	Miconazole
Fusarium Lini	–	30%	–	–	Miconazole

The (–) sign indicates no inhibition against fungi

Table 6: Results of antibacterial activities of polymers in DMSO Solvent

Bacteria	% inhibition of polymers compared with the % inhibition of standard drug Ofloxacin				
	P*p*HOBND	P*p*HOBPD	P*p*HOBCy	P*o*HOBPD	P*o*HOBP
Escherichia Coli	10.936	7.180	3.249	–	8.865
Shigella flexeneri	–	–	–	–	–
Staphylococcus aureus	8.952	4.526	21.944	18.601	–
Psuedomonas aeruginosa	–	–	–	–	–

The (–) sign indicates no inhibition against bacteria

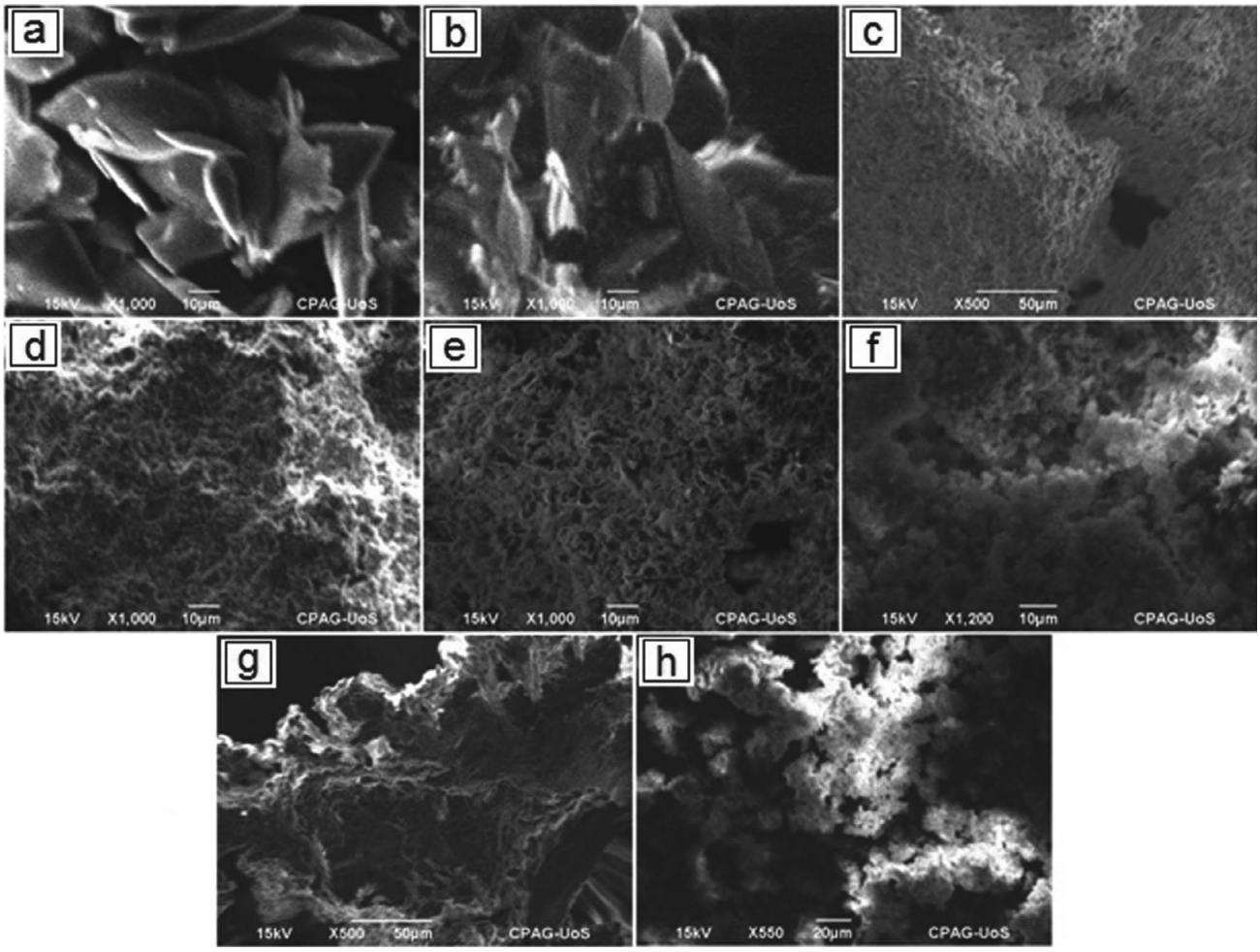

Figure 7. SEM Images of (a) *p*-HOB (b) *o*-HOB (c) P*p*HOBND (d) P*p*HOBPD (e) P*p*HOBCy (f) P*o*HOBPD (g) P*o*HOBP and (h) Schiff base reported[34] conditions as experimental.

3. 10. Scanning Electron Microscopy of Monomers and Polymers

The SEM images of the monomers and polymers were recorded at 100, 50, 20 and 10 μm. The polymer P*p*HOBND and P*p*HOBPD had sponge like morphology (Figure 7c and 7d). The polymer P*p*HOBCy had fibrous like clusters with porous surface (Figure 7e). The morphology of polymer P*o*HOBPD was agglomerated and this agglomerated structure was due to inter-particle attraction of monomers (Figure 7f). P*o*HOBP had nanoscale roughness (Figure 7g) while the reported Schiff base derived from *o*-HOB[34] had agglomerated clusters (Figure 7h). The monomer *p*-HOB had seeds like morphology (Figure 7a) and the monomer *o*-HOB had leaves like appearance (Figure 7b). The results support that the morphology of the polymers was different from their corresponding monomers.

4. Conclusion

Five new photo-responsive polyazomethines with flexible spacers of n-hexane were synthesized by one step polycondensation between dialdehydes and diamines. The polymers were characterized by elemental microanalysis, UV-Vis, fluorescence, FT-IR, ^{1}HNMR, TG/DTA and SEM. The polymers indicated fluorescence emissions within visible region with LODs of polymers at 0.625–1.25 μg/ml levels and high thermal stabilities within the range of 412–708˚C. The polymers were also tested for their antimicrobial activities against bacteria and fungi, the polymer P*p*HOBND indicated moderate antifungal activity against Aspergillus nigar.

5. References

1. G. F. D'Alelio, in: N. M. Bikales (Ed.): Encyclopedia of Polymer Science and Technology, Vol.10, Interscience, New York, **1969,** pp. 659.
2. S. Banerjee, C. Saxena, *J. Polym. Sci. A Polym. Chem*. **1996,** *34*, 3565–3572. **DOI:**10.1002/(SICI)1099-0518(199612)34:17<3565::AID-POLA11>3.0.CO;2-C
3. A. G. EI-Shakeil , M. K. H. Saad-Addin, A. A. Dheya, Polymer Bulletin. **1997**, *39*, 1-7. **DOI:**10.1007/s002890050112
4. M. Y. Khuhawar, M. A. Mughal, A. H. Channar, *Eur. Polym. J*. **2004**, *40*, 805–809. **DOI:**10.1016/j.eurpolymj.2003.11.020
5. A. Iwan, *Sustainable Energy Rev*. **2015,** *52*, 65–79. **DOI:**10.1016/j.rser.2015.07.078
6. M. L. Petrus, R. K. M. Bouwer, U. Lafont, D. H. K. Murthy, R. J. P. Kist, M. L. Böhm, Y. Olivier, T. J. Savenije, L. D. A. Siebbeles, N. C. Greenham, T. J. Dingemans, *Polym. Chem*. **2013**, *4*, 4182-4191. **DOI:**10.1039/C3PY00433C
7. A. Iwan, M. Palewicz, A. Sikoran, J. Chmielowiec, A. Hreniak, G. Pasciak, P. Bilski, *Synth Met*. **2010,** *160*, 1856-1867. **DOI:**10.1016/j-synthmet.2010.06.029
8. D. Sek, B. Jarzabek, E. Grabiek, B. Kaczmarczyk, H. Janeczek, A. Sikora, A. Hreniak, M. Palewicz, M. Lapowski, K. Karon, A. Iwan, *Synth Met*. **2010**, *160*, 2065-2076. **DOI:**10.1016/j.synthmet.2010.07.026
9. P. K. Dutta, P. Jain, P. Sen, R. Trivedi, P. K. Sen, J. Dutta, *Eur. Polym. J.* **2003**, *39*, 1007–1011. **DOI:**10.1016/S0014-3057(02)00328-2
10. V. Cozan, E. Butuc, A. Stoleriu, M. Rusa, M. Rusu, Y. Ni, M. DING, *J. Macromol. Sci.-Pure Appl. Chem.* **1995,** *32*, 1243–1262.
11. V. Cozan, L. Marin, in: M. Cazacu (Ed.): Thermotropic Liquid Crystalline Polyazomethines, in Advances in Functional Heterochain Polymers, Chapter 3, Nova Publishers Inc., New York, **2008**, ISBN 978-1-60456-598-0, pp. 67-115.
12. S. Ogiri, M. Ikeda, A. Kanazawa, T. Shiono, T. Ikeda, *Polymer*. **1999**, *40*, 2145–2150. **DOI:**10.1016/S0032-3861(98)00421-2
13. C-H. Li, T-C. Chang, *J. Polym. Sci. A Polym. Chem*. **1990**, *28*, 3625–3638. **DOI:**10.1002/pola.1990.080281309
14. A. Iwan, E. Schab-Balcerzak, D. Pociecha, M. Krompiec, M. Grucela, P. Bilski, M. Klosowski, H. Janeczek, *A Polym. Chem*. 2011, *34*, 61–74. **DOI:**10.1016/j.optmat.2011.07.004
15. A. Iwan, B. Boharewicz, I. Tazbir, M. Malinowski, M. Filapek, T. Kłąb, B. Luszczynska, I. Glowacki, K. P. Korona, M. Kaminska, J. Wojtkiewicz, M. Lewandowska, A. Hreniak, Solar *Energy*. **2015**, *117*, 246-259. **DOI:**10.1016/j.solener.2015.03.051
16. A. Iwan, B. Boharewicz, I. Tazbir, M. Filapek, *Electrochim. Acta*. **2015**, *159*, 81–92 **DOI:**10.1016/j.electacta.2015.01.215
17. A. Iwan, B. Boharewicz, I. Tazbir, A. Sikora, M. Maliński, Ł. Chrobak, W. Madej, *Chem. Sci Rev. Lett*. **2015**, *4*, 597-608
18. A. Iwan, E. Schab-Balcerzak, K. P. Korona, S. Grankowska, M. Kamińska, *Synth Met*. **2013**, *185–186*, 17–24. **DOI:**10.1016/j.synthmet.2013.10.008
19. M. A. Mughal, A. H, Mughal, Z. M. Ali, G.Z. Memon, M. Y. Khuhawar, H. Saleem, *IOSR, Journal of Engineering (IOSRJEN)*. **2013**, *3*, 48–55
20. N. Nishat, R. Rasool, S. Parveen, S.A. Khan, *J. Appl. Polym. Sci*. **2011**, *122*, 2756–2756. **DOI:**10.1002/app.34100
21. I. A. Alkskas, A. M. Alhubge, F. Azam, *Chin. J. Polym. Sci*. **2013,** *31*, 471–480. **DOI:**10.1007/s10118-013-1237-4
22. N. Y. Baran, M. Karakşla, H. Ö Demir, M. Saçak, *J Mol Struct*. **2016**, *1123*, 153–161. **DOI:**10.1016/j.molstruc.2016.06.028
23. L. Guo, S. Wu, F. Zeng, J. Zhao, *Eur. Polym. J*. **2006**, *42*, 1670–1675. **DOI:**10.1016/j.eurpolymj.2006.01.025
24. M. K. Choi, H. L. Kim, D. H. Suh, *J. Appl. Polym. Sci*. **2006**, *101*, 1228–1233. **DOI:**10.1002/app.24209
25. A. Shah, M. Y. Khuhawar, A. A. Shah, *J. Appl. Polym. Sci*. **2012**, *21*, 325–334. **DOI:**10.1007/s13726-012-0033-2
26. O. Catanescu, M. Grigoras, G. Colotin, A. Dobreanu, N. Hurduc, C.I. Simionescu, *Eur. Polym. J.* **2001**, *37*, 2213–2216. **DOI:**10.1016/S0014-3057(01)00119-7
27. O. Thomas, O. Inganäs, M. R Andersson, *Macromolecules*. **1998**, *31*, 2676–2678. **DOI:**10.1021/ma9701090
28. P. K. Gutch, S. Banerjee, D. C. Gupta, D. K. Jaiswal, *Polym. Chem*. **2001**, *39*, 383–388. **DOI:**10.1002/1099-0518(20010201)39:3<383::AID-POLA1005>3.0.CO;2-3

29. Y-l. Wang, G. Zhang, M-l. Zhang, Y. Fan, B-y. Liu, J. Yang, *Chin. J. Polym. Sci*. **2012**, *30*, 370–377. **DOI:**10.1007/s10118-012-1124-4
30. S. Shi, Z. Li, J. Wang, *J POLYM RES*, **2007**, *14*, 305–312. **DOI:**10.1007/s10965-007-9111-0
31. F. Qureshi, M. Y. Khuhawar, T. M. Jahangir, A. H. Channar, *Acta Chim. Slov*. **2016**, *63*, 113–120. **DOI:**10.17344/acsi.2015.1994
32. H. B. Donahoe, L. E. Benjamin, L. V. Fennoy, D. Greiff, *J. Org. Chem*. **1961**, *26*, **DOI:**10.1021/jo01061a047
33. R. W. Date, C. T. Imrie, G. R. Luckhurst, J. M. Seddon, *Liquid Crystals*, **1992**, *12*, 203–238. **DOI:**10.1080/02678299208030393
34. S. İlhan, H. Temel, M. Sunkur, İ. Teğin, *Indian Journal of Chemistry*, **2008,** *47A*, 560–564.

Povzetek

Pet novih azometinskih polimerov, ki imajo alifatsko-aromatske dele, smo sintetizirali s polikondenzacijo dialdehidov in diaminov. Dialdehidni monomeri se razlikujejo le po orientaciji aromatskega obroča (orto ali para) in so bili sintetizirani s kondenzacijsko reakcijo med aromatskim aldehidom in 1,6-dibromoheksanom. Molekulsko maso monomerov smo določili z masno spektroskopijo z ionizacijo z elektroni (EI). Strukture polimerov smo potrdili z elementarno mikroanalizo, infrardečo spektroskopijo (FTIR), NMR spektroskopijo (1HNMR) in UV-VIS spektroskopijo. Morfologijo monomerov in polimerov smo ocenili z vrstično elektronsko mikroskopijo (SEM). Vsi polimeri so bili topni v DMSO (pri segrevanju) in nekoliko v drugih topilih. Termično stabilnost polimerov smo analizirali s termogravimetrično analizo (TG) in diferenčno termično analizo (DTA). Toplotna stabilnost polimeriv je bila višja od njihovih ustreznih monomerov. TG polimerov je pokazala najvišjo stopnjo izgube mase (T_{max}) v območju od 412 °C do 708 °C. S fluorescenčno emisijsko spektroskopijo polimerov smo pokazali, da vsi polimeri fluorescirajo in določili od enega do štirih emisijskih vrhov v območju od 349 nm do 606 nm. Meja detekcije polimerov je bila v območju od 0,625 μg/ml do1,25 μg/ml. Polimerom smo določali tudi njihovo protimikrobno aktivnost napram bakterijam in glivam.